Sparse regularization for least-squares AVP migration

Juefu Wang and Mauricio D. Sacchi, Department of Physics, University of Alberta

2005 CSEG National Convention

Abstract

This paper presents least-squares wave equation AVP (Amplitude versus Ray Parameter) migration with non-quadratic regularization. We pose migration as an inverse problem and propose a cost function that makes use of *a priori* information about the AVP common image gather. In particular, we introduce two regularization goals: smoothness along the ray parameter direction and sparseness in the depth direction. The latter yields a high-resolution AVP gather with robust estimates of amplitude variations with ray parameter. An iterative re-weighted least-squares conjugated gradients algorithm minimizes the cost function. We test the algorithm by solving a multi-channel deconvolution problem and a 2-D wave equation AVP migration problem. We also discuss the difficulties and a potential pitfall of this new imaging scheme.

Introduction

In seismic exploration, we are often interested in two types of information about an earth model: structural information and rock property parameters. For structural imaging, this is emphasized by improving the spatial resolution. In recent years, much attention has been paid to high-resolution structural imaging algorithms. At the same time, with the development of AVO technologies, geophysicists are more and more interested in amplitude-preserving migration/inversion methods. It has been shown (Nemeth et al., 1999; Duquet et al., 2000; Kuehl, et al., 2002, 2003) that seismic resolution can be improved by inverting the De-migration/Migration kernel and by enforcing a regularization constraint, for example, by introducing smoothness in the solution. However, as the results of these methods show, there are many artifacts present in the solution due to operator mismatch, wave-field sampling and noise.

One possible way to further enhance the resolution and attenuate artifacts is by taking advantage of the solution itself. Iteratively using the result as model-space regularization can lead to high-resolution artifact-free seismic images. This idea has been used in many fields of signal processing (Sacchi and Ulrych, 1995; Charbonnier, et al., 1997; Youzwhisen, 2001; Sacchi, et al., 2003; Trad et al., 2003; Downtown and Lines, 2004.). In this paper, we utilize a model-dependent sparse regularization and a model-independent smoothing regularization for an AVP imaging problem. The first regularization arises from an update of the stacked image, and the second regularization is implemented via a convolutional operator applied to AVP common image gathers along the ray parameter direction. With such regularization strategy, we try to develop an algorithm to simultaneously improve the structural interpretability and amplitude accuracy of seismic images.

Methodology

Regularization is very important for inversion since it takes advantage of *a prior* information of the model, and it allows us to efficiently solve ill-posed problems. For example, Kuehl and Sacchi (2002, 2003) showed that applying smoothing regularization in ray-parameter direction can help to remove artifacts introduced by missing information, aliasing, noise and operator mismatch. The scheme is based on the minimization of a quadratic cost function. Sacchi et al. (2003) showed that higher solution can be acquired by solving a non-quadratic problem. In this paper we reformulate the cost function for least-squares wave-equation AVP/AVA migration problem as follows:

$$J(m) = \| W(Lm - d) \|_2^2 + \lambda^2 \| F(SDm) \|, \qquad (1)$$

where m is the earth model, AVP common image gathers, L is a wave-equation based modeling operator that transforms the model to seismic data, d is the seismic data, and W is a sampling matrix to simulate the geometry of data acquisition. D is a model-independent high-pass filter to penalize non-smooth solutions, S is a stacking operator that converts common image gathers to the stacked image, F is a model-dependent function used to enforce sparseness, and λ is a trade-off parameter to control the amount of regularization . By using Cauchy norm (Sacchi and Ulrych, 1995), the sparse regularization operator F can be formulated as the following:

$$F(m) = \sum_{i=1}^{n} \ln(1 + m_i^2 / \sigma_m{}^2), \quad (2)$$

where $\sigma_m{}^2$ is a scale parameter. By adopting a preconditioning strategy (Wang, et al., 2004) , the cost function can be recast as bellow:

$$J(z) = \| W(LPz - d) \|_2^2 + \lambda^2 \| F(Sz) \|, \quad (3)$$

where P is the preconditioner, and z is the model modified by the preconditioner. Here we use a Hamming window as P to remove artifacts and fill in gaps of neighboring amplitudes. Obviously, the final solution is $m = Pz$. The problem can be efficiently solved by Iterative Re-weighted Least-squares algorithm (IRLS) (Scales and Smith, 1994). The cost function of *k* th iteration of IRLS algorithm is:

$$J(z_k) = \| W(LPz_k - d) \|_2^2 + \mu^2 \| \sqrt{Q_{k-1}} Sz_k \|_2^2, \quad (4)$$

where Q_{k-1} is a diagonal weighting matrix, its diagonal elements are calculated by

$$Q_{ii}^{k-1} = \frac{1}{1 + (m_{si}^{k-1} / \sigma_{ms}^{k-1})^2},$$

where m_{si}^{k-1} is the *i* th element of the vector *Sz* at (*k-1*) th iteration of IRLS, and σ_{ms}^{k-1} is a scale parameter, which is empirically set to some percentage of the maximum amplitude of the mentioned vector. Please note that some scaling factor has been absorbed into the trade-off parameter μ . IRLS for the above problem is applied in the following way. First, we initialize *m* with zeros and *Q* with an identity matrix. Then we minimize cost function (3) via the CG algorithm. We then update the diagonal matrix, and restart the CG algorithm. We repeat this procedure for a few updates (4-5 iterations) until sparsity in the vertical direction has been achieved. In a few words, IRLS contains two loops. The inner loop is the CG iteration, and the outer loop is the update of the weighting matrix.

A toy example: multi-channel deconvolution

We tested the idea of forcing sparseness and smoothness at the same time by a simple multi-channel deconvolution problem. This is an unrealistic scenario in seismic deconvolution but yet it is a good example to test our algorithm. The procedure, however, could be used to deconvolve time-migrated common image gathers. Figure 1a is a time domain model with 20 offsets. We convolve the model with a zero-phase wavelet, and mute three offsets (trace number equals 2, 6 and 9) to also test the procedure in situations of missing information. The data are portrayed in Figure 1b.

We compared two methods of inversion, preconditioned LS inversion (Wang et al. , 2004) and sparse LS inversion (proposed in this paper). Figure 1c is the result of the precondioned LS inversion after 50 iterations of the CG algorithm. It is evident that the inversion successfully fill in the gap in the incomplete data. However, the vertical resolution is not satisfactory. Spurious sidelobes are present in the inverted reflectivity model. On the other hand, the sparse inversion provides a superior result (Figure 1d). It is almost identical to the real reflectivity model. The wavelet has been properly compressed. In addition, the AVO signature has been preserved.

A 2-D synthetic example: Sparse LS Migration

We prepared a set of 2D synthetic data to test the sparse least-squares migration. The model for the data set consists of four flat layers and a half-space. We use a ray tracer that accounts for the correct reflector AVA, cylindrical divergence (line sources), and interface transmission losses in a laterally invariant earth model. Each CMP gather has 61 offsets with a spacing of 25m. 10 CMP gathers are produced with a spacing of 25m. Then we randomly removed 70% of the traces to simulate a very sparse 2D survey.

We compared three methods of 2-D AVA imaging, conventional migration (the adjoint of modeling operator), preconditioned least-squares migration (PLSM) and sparse least-squares migration (SLSM, proposed in this paper). Figure 2 displays a zoomed view of three common image gathers produced by these methods. It is clear that both PLSM and SLSM provide much better result than conventional method. Artifacts are efficiently removed by the algorithms. SLSM provides a solution with higher resolution than PLSM. The method has the ability of suppressing the sidelobes introduced by the band-limited nature of the data. To complete our analysis, we have extracted the amplitude of the first event and plotted AVA curves for three methods in Figure 3. It can be seen that SLSM slightly improves the peak amplitude within the invertible angle range. Figure 4 compares the stacked images for three methods. It is

clear that PLSM better resolves the image than conventional migration, but some artifacts are still present. On the other hand, SLSM suppresses these artifacts by forcing sparseness in the vertical direction. However, the improvement is not so impressive as in the deconvolution example that we have shown in the previous section. Two reasons may account for this observation. First is the ubiquitous problems of operator mismatch (the forward operator utilized in LS migration is an approximation to the operator used to generate the synthetic wavefields). The second is the wavelet distortion introduced by the conversion from time domain (data) and depth domain (model).

Conclusions and discussion

SLSM slightly improves the accuracy of amplitude of image gathers. At the same time, the algorithm removes spurious artifacts during inversion by forcing a gradually updated diagonal weighting. It might be expensive to apply SLSM due to the requirement of two optimal trade-off parameters. Furthermore, tests on data generated with more complex earth models are necessary to confirm the validity of this method. In some of our tests we found that over regularization leads to loss of valuable information that is contained in events with small amplitudes. This is a potential pitfall of SLSM. This a problem also encountered in popular techniques for post-stack inversion of seismic data that are based on the sparse reflectivity assumption.

Acknowledgements

We would like to acknowledge financial support from the following companies: GeoX Ltd., EnCana Ltd., Veritas GeoServices and the Schlumberger Foundation. The research has also been supported by NSERC via a grant to M.D.Sacchi.

References

Charbonnier, P., Blanc-Feraud, L., et al., 1997, Deterministic edge-preserving regularization in computed imaging: IEEE Transactions on Image Processing, **6**, 298-311.

Downtown, J. and Lines, L., 2004, Three term AVO waveform inversion, CSEG annual convention, Abstracts, 5 pages, CDROM

Duquet, B., Marfurt, K. J. and Dellinger, J. A., 2000, Kirchhoff modeling, inversion for reflectivity, and subsurface illumination: Geophysics, **65**, 1195-1209.

Kuehl, H., and Sacchi, M.D., 2002, Robust AVP estimation using least-squares wave-equation migration: 72nd Annual Mtg., Soc. Expl. Geopl., Expanded Abstracts, 4 pages, CDROM.

Kuehl, H., and Sacchi M.D., 2003, Least-squares wave-equation migration for AVP/AVA inversion: Geophysics, **68**, 262-273.

Nemeth, T., Wu, C. and Schuster, G. T., 1999, Least-squares migration of incomplete reflection data: Geophysics, **64** 208-221.

Sacchi, M.D., and Ulrych, T.J., 1995, High resolution velocity gathers and offset space reconstruction: Geophysics, **60**, 1169-1177.

Sacchi, M. D., Constantinescu, C. M. and Feng, J., 2003, Enhancing resolution via non-quadratic regularization-next generation of imaging Algorithms: CSEG Annual Convention. CDROM, 5 pages.

Scales, J. A. and Smith, M. L., 1994, Introductory geophysical inverse theory: Samizdat Press.

Trad, D., Ulrych, T. and Sacchi, M. D., 2003, Latest views of the sparse Radon transform: Geophysics: **68**, 386-399.

Wang, J., Kuehl, H. and Sacchi, M. D., 2004, Preconditioned least-squares wave-equation AVP migration, CSEG Annual Convention, CDROM, 3 pages.

Youzwishen, C., 2001, Non-linear sparse and blocky constrains for seismic inverse problems, Msc. thesis: University of Alberta.

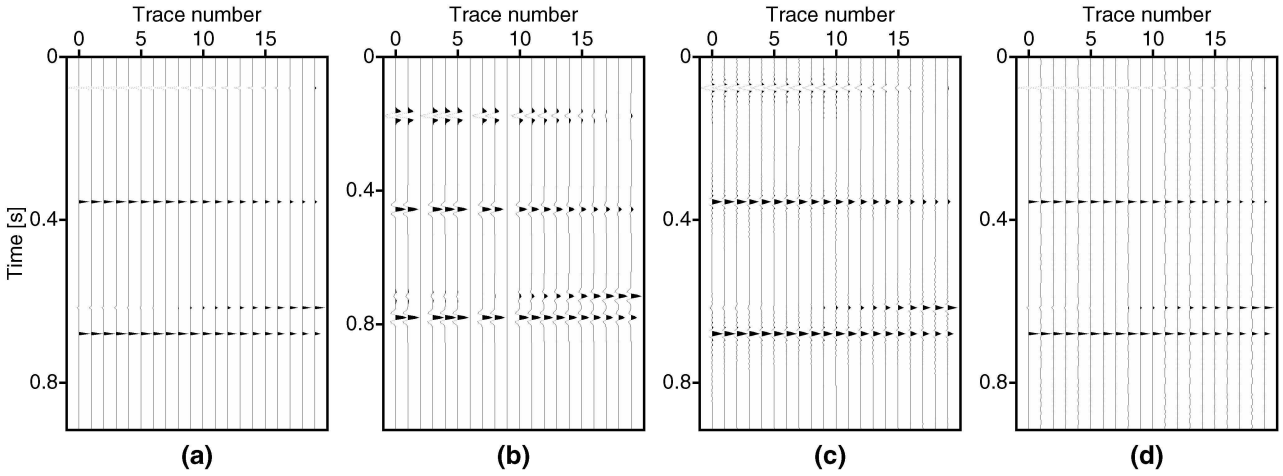

E Figure 1 A multi-channel deconvolution example to compare linear inversion and non-linear inversion. (a) Reflectivity model. (b) Incomplete multi-channel data. (c) Linearly inverted model. (d) Non-linearly inverted model (sparse solution).

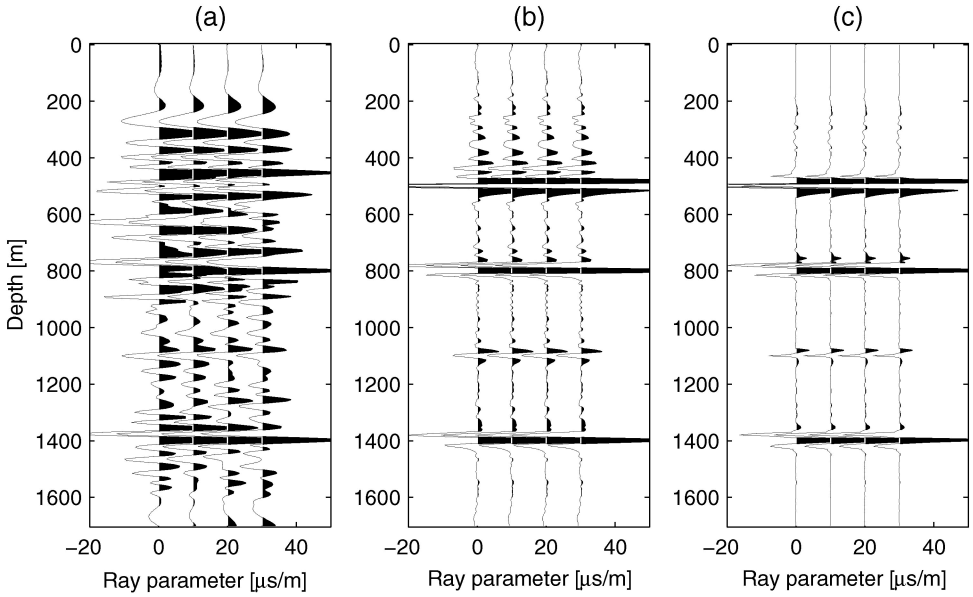

Figure 2 Zoomed view of common image gathers produced by migration (a), PLSM (b) and SLSM (c). Only first four traces of each image gathers are displayed.

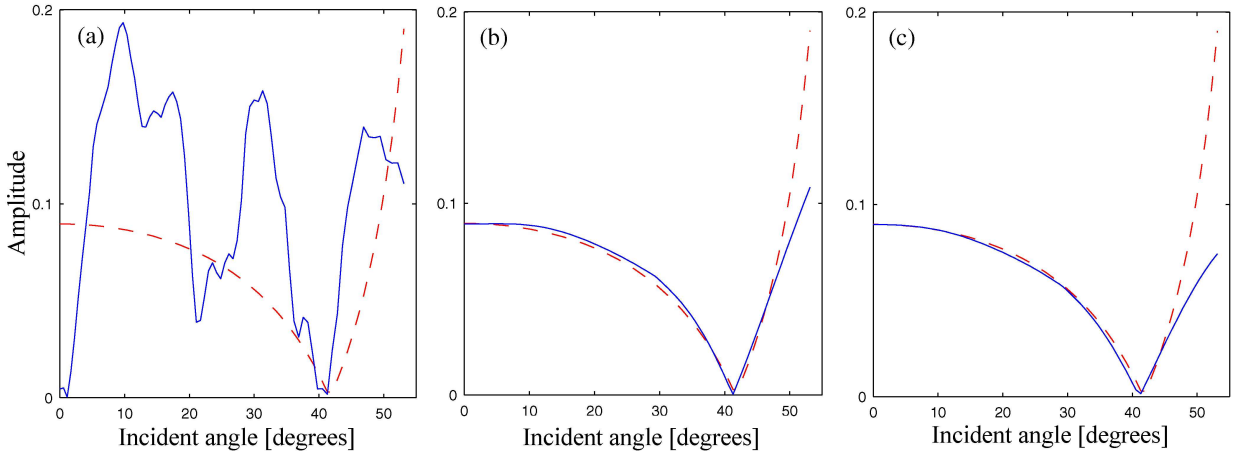

Figure 3 AVA curves for the first event of common image gathers produced by migration (a), PLSM (b) and SLSM (c). Blue solid curves: inverted AVA; Red dashed curves: theoretical curves.

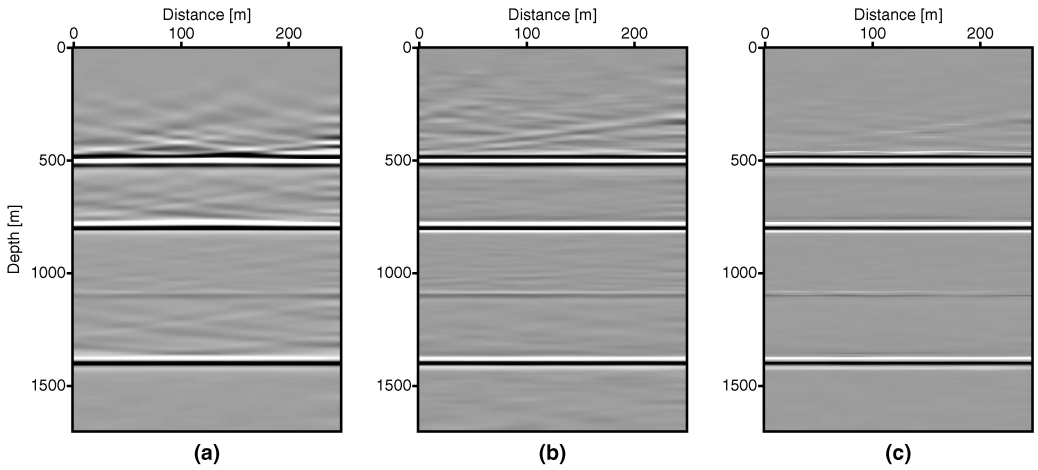

Figure 4 Stacked images from migration (a), PLSM (b) and SLSM (c).